European Journal of Medicinal Chemistry 46 (2011) 1147–1152

Contents lists available at ScienceDirect

European Journal of Medicinal Chemistry

journal homepage: http://www.elsevier.com/locate/ejmech

Original article

Synthesis, human monoamine oxidase inhibitory activity and molecular docking studies of 3-heteroarylcoumarin derivatives

Giovanna Delogu [a], Carmen Picciau [a], Giulio Ferino [b], Elías Quezada [c], Gianni Podda [a], Eugenio Uriarte [b], Dolores Viña [d,*]

[a] Dipartimento Farmaco Chimico Tecnologico, Universita degli Studi di Cagliari, Via Ospedale 72, 09124 Cagliari, Italy
[b] Departamento de Química Orgánica, Facultad de Farmacia, Universidad de Santiago de Compostela, 15782 Santiago de Compostela, Spain
[c] Departamento de Química, Facudade de Ciências, Universidade de Porto, 4169-007 Porto, Portugal
[d] Departamento de Farmacología, Facultad de Farmacia, Universidad de Santiago de Compostela, Campus Vida, 15782 Santiago de Compostela, Spain

ARTICLE INFO

Article history:
Received 30 September 2010
Received in revised form
12 January 2011
Accepted 18 January 2011
Available online 28 January 2011

This article is dedicated to the memory of Prof. Francisco Orallo.

Keywords:
3-Heteroarylcoumarins
Perkin reaction
Monoamino oxidase (MAO)
Molecular docking

ABSTRACT

Monoamine oxidase (MAO) is an important drug target for the treatment of neurological disorders. Series of 3-indolyl and 3-thiophenylcoumarins were synthesized and evaluated as inhibitors of the two human MAO isoforms, hMAO-A and hMAO-B. In general, the derivatives were found to be selective hMAO-B inhibitors with IC_{50} values in the nanoMolar (nM) to microMolar (μM) range. Docking experiments were carried out in order to compare the theoretical and experimental affinity of these compounds to the hMAO-B protein. According to our results, docking experiments could be an interesting approach to try to predict the activity of this class of coumarins against MAO-B receptors.

1. Introduction

MAO is a FAD-containing enzyme with two known isoforms (MAO-A and MAO-B) and it is present in the outer membrane of mitochondria in glial, neuronal and many other cells [1]. Deamination of adrenaline, noradrenaline and serotonin is catalyzed by MAO-A whilst deamination of β-phenylethylamine and benzylamine is catalyzed by MAO-B [2]. The MAO metabolic reaction involves the oxidation of the amine functional group via oxidative cleavage of the α-CH bond of the substrate with the ensuing generation of an imine intermediate. This pathway is accomplished by the reduction of the flavin cofactor that is reoxidized by molecular oxygen, with simultaneous hydrogen peroxide release. Subsequently, the imine intermediate is hydrolyzed by a non-enzymatic pathway yielding ammonia and the corresponding aldehyde [3]. This enzymatic function decreases the synaptic concentration of the neurotransmitters mentioned above and controls a great extent the neurone's excitement in those possessing receptors for these mediators [4]. These properties determine the clinical importance of MAO inhibitors. In fact, interest in selective MAO-B inhibitors has increased in recent years due to their therapeutic potential in aging related neurodegenerative diseases such as Alzheimer's disease (AD) and Parkinson's disease (PD) [5]. Selective MAO-A inhibitors have been used because of their therapeutic potential as antidepresants [6].

The recent description of the crystal structure of the two isoforms of hMAO helps us to elucidate the underlying mechanisms. It allows us to investigate the selective interactions between these proteins and their ligands. It also allows us to probe the catalytic mechanism, helping us to gain a complete understanding of the pharmacophoric requirements necessary for the rational design of new inhibitors [7,8].

Among the different existing inhibitors, those with a (1*H*)-benzopyran structure have been deeply studied [9]. Substitution of the coumarin nucleus at position 3 has been carried out with phenyl, methyl, carboxylic acid, ethyl esther or acyl chloride groups [10]. Our research group has reported in several studies, the importance to the MAO inhibitory activity of different substituents on the phenyl ring, in the position 3 of the coumarin [11–13]. In this work we synthesized and tested for MAO inhibitory activity some coumarin

* Corresponding author. Tel.: +34 981563100; fax: +34 981594595.
E-mail address: mdolores.vina@usc.es (D. Viña).

0223-5234/$ – see front matter © 2011 Elsevier Masson SAS. All rights reserved.
doi:10.1016/j.ejmech.2011.01.033

derivatives substituted at position 3 with different heterocyclic rings. Additionally, we explored the importance of the number and position of methoxy groups on (1*H*)-benzopyran structure.

2. Results and discussion

2.1. Chemistry

The 3-heteroarylcoumarin derivatives were synthesized in moderate yield (25–47%) via the classical Perkin reaction [14–17] by condensation of the *ortho*-hydroxybenzaldehydes conveniently substituted and the appropriately substituted acetic acids, using N,N′-dicyclohexylcarbodiimide (DCC) as dehydrating agent (Fig. 1). The structures of these compounds were confirmed by ^{1}H NMR, ^{13}C NMR, mass spectrometry and elemental analyses.

2.2. Enzyme inhibition studies

The potential effects of the new synthesized compounds on hMAO activity were investigated by measuring their effects on the production of hydrogen peroxide (H_2O_2) from *p*-tyramine, using the Amplex® Red MAO assay kit (Molecular Probes, Inc., Eugene, Oregon, USA) and MAO isoforms in microsomes prepared from insect cells (BTI-TN-5B1-4) infected with recombinant baculovirus containing cDNA inserts for hMAO-A or hMAO-B (Sigma–Aldrich Química S.A., Alcobendas, Spain). The inhibition of hMAO activity was evaluated using the above method following the general procedure described previously by us [18]. The test compounds did not show any interference with the reagents used for biochemical assay.

The control activity of hMAO-A and hMAO-B using *p*-tyramine as the common substrate was 165 ± 2 pmol of *p*-tyramine oxidized to *p*-hydroxyphenylacetaldehyde/min ($n = 20$).

The results of the hMAO-A and hMAO-B inhibition studies with compounds **1a**–**c**, **2a**–**c**, **3a**–**c** and **4a**–**c** are reported in Table 1 together with the selectivity index (SI hMAO-B = [IC_{50}(hMAO-A)]/[IC_{50}(hMAO-B)]). Enzymatic assays revealed that most of test compounds were moderate to potent hMAO inhibitors at either low micromolar to nanomolar concentrations, showing selectivity toward hMAO-B.

We observed that the number and position of methoxy groups on the (1*H*)-benzopyran structure is more important for hMAO activity than the nature of the heterocycle ring in position 3. In fact, compounds **4a**–**c** showing methoxy groups at positions 5 and 7 on the (1*H*)-benzopyran structure are inactive as MAO inhibitors. Introduction of a methoxy group at either position 6 or 7 on the (1*H*)-benzopyran structure, increases the MAO-B activity between 10 and 100 fold (compare **1a** vs **2a** and **3a**; **1b** vs **2b** and **3b**; **1c** vs **2c**) with the only exception being compound **3c**. Methoxy groups at position 7 (compounds **2a**–**c**) improved the MAO-B inhibitory activity compared to the corresponding compounds with the methoxy group at position 6, however compounds **2b** and **2c** showed a weak MAO-A inhibitory activity leading to a small decrease in the B-selectivity.

Table 1
IC_{50} values and hMAO-B selectivity index for the new compounds and reference inhibitors on the enzymatic activity of human recombinant MAO isoforms expressed in baculovirus infected BTI insect cells.

Compound	MAO-A (IC_{50})	MAO-B (IC_{50})	SI MAO-B
1a	**	6.37 ± 0.43 μM	>15[b]
1b	**	13.3 ± 0.89 μM	>7.5[b]
1c	**	1.92 ± 0.13 μM	>52[b]
2a	**	262.95 ± 17.61 nM	>380[b]
2b	4.16 ± 0.28 μM[a]	55.63 ± 3.73 nM	>75
2c	9.67 ± 0.65 μM[a]	45.95 ± 3.08 nM	>210
3a	**	633.55 ± 42.43 nM	>158[b]
3b	**	233.73 ± 15.65 nM	>428[b]
3c	**	**	–
4a	**	**	–
4b	**	**	–
4c	**	**	–
R-(−)-Deprenyl	67.25 ± 1.02 μM[a]	14.80 ± 0.99 nM	4544
Iproniazide	6.56 ± 0.76 μM	7.54 ± 0.36 μM	0.87

Each IC_{50} value is the mean ± S.E.M. from five experiments ($n = 5$). **Inactive at 100 μM (highest concentration tested). At higher concentrations the compounds precipitate. SI: hMAO-B selectivity index = IC_{50}(hMAO-A)/IC_{50}(hMAO-B).

[a] $P < 0.01$ *vs* the corresponding IC_{50} values obtained against MAO-B, as determined by ANOVA/Dunnett's.

[b] Values obtained under the assumption that the corresponding IC_{50} against MAO-A is the highest concentration tested (100 μM).

2.3. Molecular docking study

Docking experiments were carried out in order to compare the theoretical and experimental affinity. A graphical inspection was also made to propose the possible binding mode for the two most active MAO-B inhibitor **2b** and **2c**. The Protein Data Bank [19] (PDB) crystallographic structure of human MAO-B (PDB code 2V60) [8] was considered as the receptor for docking simulations.

The scoring function estimates the affinity between ligands and receptor [20,21]. In order to verify the usefulness of the scoring

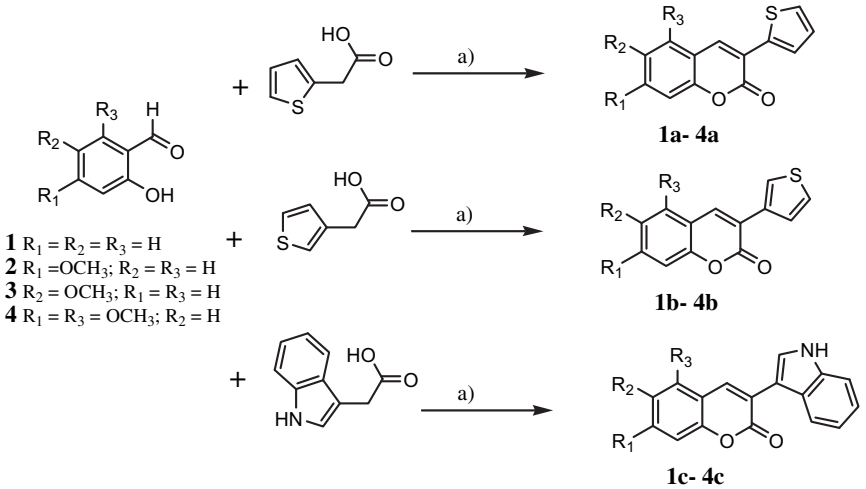

Fig. 1. Reagents and conditions: a) DCC/DMSO 110 °C, 24–48 h.

Table 2
Comparison between experimental activity and predicted scoring function against MAO-B.

Docking rank[a]	Drug	IC_{50}[b]	Docking score[c]
1	**4c**	**	−8.4274
2	**2a**	0.2630	−8.1976
3	**2c**	0.0459	−7.9367
4	**3a**	0.6335	−7.9025
5	**2b**	0.0556	−7.8267
6	**3b**	0.2337	−7.5740
7	**1c**	1.9200	−7.5170
8	**1b**	13.3000	−7.4479
9	**3c**	**	−7.2776
10	**1a**	6.3700	−6.4593
11	**4b**	**	−5.3446
12	**4a**	**	−5.1865

**Inactive at 100 μM (highest concentration tested). At higher concentrations the compounds precipitate.
[a] Docking rank taking into account the study coumarins compounds.
[b] Expressed in μM.
[c] Expressed in kJ/mol.

function to recognize new molecules potentially active as MAO-B inhibitors, different ligands were docked to the MAO-B protein.

The experimental IC_{50} values were compared with those for the predicted activity according to the scoring function (see Table 2). The square of the correlation coefficient (r^2), between the scoring function and the experimental MAO-B inhibitory activity pK_i, was calculated as 0.44. This result is reasonable considering that scoring functions are not able to provide a good correlation between the predicted and the experimental affinity [22–24]. In our case, a certain tendency of the model to rank the compounds based on their respective activity can be appreciated. In fact, when a cut-off value of $IC_{50} = 1.0$ μM is used in order to differentiate the compounds in two groups (high and low affinity), the model is able to recognize clearly both groups. The most active compounds occupy the first positions according to the scoring function. However, the compounds with $IC_{50} > 1.0$ μM, are ranked in the last positions. The only exception is the inactive coumarin **4c** which is ranked in the first positions (see Table 2).

A second study was carried out in order to assess whether the model discriminates between ligands and decoys. The synthesized coumarins were dispersed in a pool of 120 decoys extracted from the ZINC database [25]. After completing docking calculations, the data was plotted to produce a receiver operative characteristics (ROC) curve. This representation is particularly suited to illustrating the tendency of a binary model to either correctly classify the compounds or predict false positives [26–28] (see Fig. 2). The area under the curve is 0.93, indicating high predictive power for model. By using docking calculations it is possible to differentiate between true ligands and decoys (see Fig. 2).

Finally, we visually investigated the most stable configurations of our active synthesized structures. In order to obtain a more accurate model of inhibitor-enzyme interactions, the most stable binding poses of our coumarins were subjected to the MacroModel-eMBrAcE minimization module of Maestro [29]. In the eMBrAcE calculation the ligands, pre-positioned with Glide, are minimized, in turn, with the receptor.

We found two different binding patterns for 3-hetero-arylcoumarins; all the 3-thiophen substituted coumarins show the same orientation. For this reason, we focused our attention only on the binding modes of the most active compounds **2b** and **2c** with the MAO-B isoform (see Fig. 3). The MAO-B active site is known; it extends from the substrate cleft, close to the FAD cofactor, to the entrance cavity situated near the protein surface [30,31].

For the 3-thiophen structures the coumarin moiety is situated up in the cavity, leaving the methoxy group directed toward FAD. Fig. 3a illustrates the most stable configuration of **2b**. As show in the figure, **2b** occupies the entrance hydrophobic cleft formed by Phe103, Pro104, Leu164, Phe168, Leu171, Cys172, Ile199, Ile316 and Tyr326. No hydrogen bonds (H-bonds) were detected for **2b**. Conversely, good van der Waals interactions with Ile199, Phe168, Gln206 and Tyr326 were observed. Besides this, electrostatic interactions with Tyr326 and Leu164 were also evident. In the binding mode of **2c** a deep recognition of the ligand into the MAO-B active site was observed (see Fig. 3b). The indole system was placed facing the FAD cofactor in the middle between the aromatic residues Tyr398 and Tyr435. Tyr398 is involved in a double π–π stacking interaction, with phenyl and pyrrol rings respectively. A H-bond concerning the indole NH of **2c** and the N5 nitrogen of the FAD cofactor, helps to stabilize the indole moiety of the coumarin. Furthermore **2c** has strong van der Waals interactions with Gln206, Tyr326, Leu171 and Cys172.

Even, though we cannot observe a significant difference between the experimental and theoretical activity of compounds **2c** and **2b**; in this study we have tried to establish how these compounds interact differently in the MAO-B binding pocket. Docking of compound **2c**, showed that stability of this coumarin

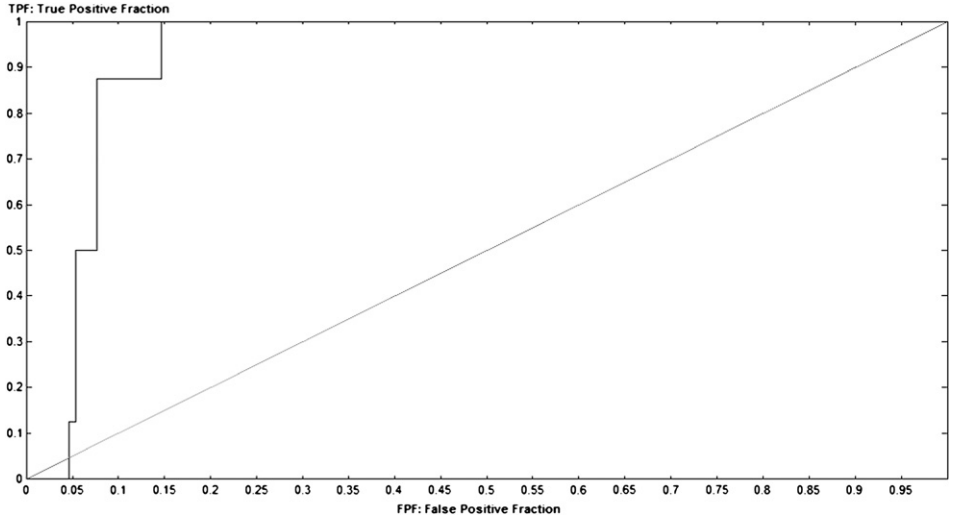

Fig. 2. ROC curve relative to synthesized coumarins and 120 ZINC decoys.

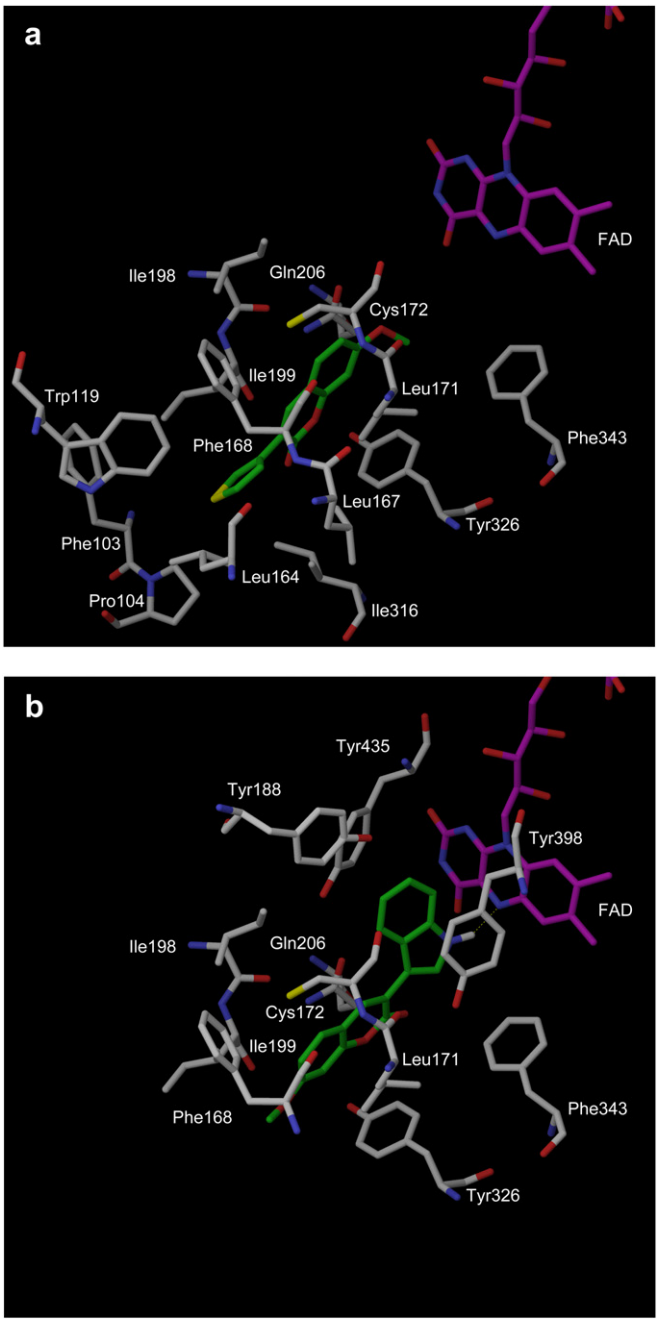

Fig. 3. Most stable binding poses of compounds **2b** (a) and **2c** (b) into the MAO-B binding pocket (PDB code: 2V60). For clarity only interacting residues, labeled in white wire, are displayed. Ligands and FAD cofactor are depicted in tube; carbon atoms are colored in green and purple for ligand and FAD respectively. In (a) all hydrogens atoms are omitted. In (b) only the hydrogen atom forming H-bond, displayed in yellow dot line, is maintained. (For interpretation of the references to colour in this figure legend, the reader is referred to the web version of this article.)

into the binding site, is due both to H-bonds formed with the FAD cofactor, aromatic rings interactions, and van der Walls forces. For **2b** instead, we can appreciate that the ligand-receptor complex is stabilized not so deeply into the binding cleft through van der Waals forces and electrostatic interactions.

3. Conclusions

In the current study, three series of 3-heteroarylcoumarin derivatives were synthesized and evaluated as inhibitors of MAO-A and -B. In general, the derivatives were found to be selective for the MAO-B isoform with 7-methoxy-3-heteroarylcoumarins exhibiting inhibition potencies in the low nanoMolar range. Docking experiments showed that the affinity of the studied compounds to MAO-B is similar to that obtained experimentally.

According to our results, docking experiments could be an interesting approach to try to predict the activity for this class of coumarins in MAO-B receptor. Moreover, the two different binding patterns for **2b** and **2c** proposed in this work, could help us to better understand the modes of interaction of new 3-heteroarylcoumarins.

4. Experimental

4.1. General methods

Melting points (mp) are uncorrected and were determined with a Reichert Kofler thermopan or in capillary tubes in a Buchi 510 apparatus. ^{1}H NMR (300 MHz) and ^{13}C NMR (75.4 MHz) spectra were recorder with a Bruker AMX spectrometer. Chemical shifts (δ) are expressed in parts per million (ppm) using TMS as an internal standard. Spin multiplicities are given as s (singlet), d (doublet), dd (doublet of doublets) and m (multiplet). Mass spectrometry was carried out with a Kratos MS-50 or a Varian MAT-711 spectrometer. Elemental analyses were performed by a Perkin–Elmer 240B microanalyzer and were within ±0.4% of calculated values in all cases. Flash Chromatography (FC) was performed on silica gel (Merck 60, 230–400 mesh); analytical TLC was performed on precoated silica gel plates (Merck 60 F_{254}).

4.2. Synthesis

4.2.1. General synthetic method for the coumarin skeleton

A solution of *ortho*-hydroxybenzaldehyde (**1**–**4**, 8 mmol), substituted acetic acid (**a**–**c**, 10 mmol) and DCC (12 mmol) in dimethylsulfoxide (DMSO, 10 mL), was heated (oil bath) at 110 °C for 24–48 h. On completion of the reaction, cold water (100 mL) and acetic acid (15 mL) were added. The reaction mixture was stirred at room temperature for 4 h and extracted with diethyl ether (4 × 100 mL). The precipitated dicyclohexylurea was filtered off. The filtrate was extracted with 5% aqueous $NaHCO_3$ (200 mL). The organic phase was stirred for 1 h with 5% aqueous sodium metabisulfite in order to remove the unreacted hydroxybenzaldehyde. The organic phase was washed with water, dried (Na_2SO_4) and the solvent removed under reduced pressure. The residue was purified by column chromatography (Hexane/EtOAc, 9:1).

4.2.2. 3-(Thiophen-2-yl)coumarin (**1a**) [29]

Yield 34%; mp 166–167 °C. ^{1}H NMR (300 MHz) ($CDCl_3$): δ = 7.12 (m, 1H), 7.28 (d, J = 9.4 Hz, 1H), 7.35 (d, J = 9.4 Hz, 1H), 7.42 (d, J = 5.1 Hz, 1H), 7.52 (m, 2H), 7.80 (d, J = 3.8 Hz, 1H), 7.99 (s, 1H). ^{13}C NMR (75.4 MHz) ($CDCl_3$): δ = 116.4, 119.3, 121.7, 124.6, 127.0, 127.5, 127.7, 129.6, 131.1, 135.5, 135.9, 152.6, 160.1. EI-MS (m/z): 229 $[M+1]^+$, 228 $[M^+]$. Anal. Calcd. for $C_{13}H_8O_2S$: C 68.40, H 3.53; Found: C 68.52, H 3.59.

4.2.3. 3-(Thiophen-3-yl)coumarin (**1b**) [32]

Yield 37%; mp 175–176 °C. ^{1}H NMR (300 MHz) ($CDCl_3$): δ = 7.30 (d, J = 7.5 Hz, 1H), 7.35 (m, 2H), 7.53 (m, 3H), 7.93 (s, 1H), 8.18 (d, J = 3.0 Hz, 1H). ^{13}C NMR (75.4 MHz) ($CDCl_3$): δ = 116.3, 119.4, 122.6, 124.5, 125.6, 126.0, 126.2, 127.7, 131.1, 134.3, 137.2, 152.8, 160.0. EI-MS (m/z): 229 $[M+1]^+$, 228 $[M^+]$. Anal. Calcd. for $C_{13}H_8O_2S$: C 68.40, H 3.53; Found: C 68.50, H 3.6.

4.2.4. 3-(Indol-3-yl)coumarin (**1c**)

Yield 33%; mp 190–191 °C. ^{1}H NMR (300 MHz) ($CDCl_3$): δ = 7.32 (m, 3H), 7.48 (m, 2H), 7.58 (dd, J = 7.6; 1.3 Hz, 1H), 7.98 (m, 1H); 8.16

(s, 1H), 8.20 (d, $J = 2.6$ Hz, 1H), 8.65 (br; 1H). ^{13}C NMR (75.4 MHz) ($CDCl_3$): $\delta = 111.9, 116.3, 119.5, 120.2, 120.9, 122.7, 122.9, 124.4, 125.5, 127.2, 127.6, 130.1, 134.9, 136.2, 143.5, 152.2, 160.8$. EI-MS ($m/z$): 262 $[M + 1]^+$, 261 $[M^+]$. Anal. Calcd. for $C_{17}H_{11}NO_2$: C 78.15, H 4.24; Found: C 78.20, H 4.30.

*4.2.5. 7-Methoxy-3-(thiophen-2-yl)coumarin (**2a**) [33]*

Yield 27%; mp 155–156 °C. ^{1}H NMR (300 MHz) ($CDCl_3$): $\delta = 3.89$ (s, 3H), 6.85 (s, 1H), 6.88 (d, $J = 8.4$ Hz, 1H), 7.11 (m, 1H), 7.38 (dd, $J = 4.0$; 1.0 Hz, 1H), 7.45 (d, $J = 8.4$ Hz, 1H), 7.74 (dd, $J = 4.0$; 1.0 Hz, 1H), 7.96 (s, 1H). ^{13}C NMR (75.4 MHz) ($CDCl_3$): $\delta = 55.8, 100.4, 112.9, 113.1, 126.1, 126.5, 126.8, 127.4, 128.7, 136.0, 136.4, 154.5, 161.0, 162.5$. EI-MS ($m/z$): 259 $[M + 1]^+$, 258 $[M^+]$. Anal. Calcd. for $C_{14}H_{10}O_3S$: C 65.10, H 3.90; Found: C 65.17, H 3.96.

*4.2.6. 7-Methoxy-3-(thiophen-3-yl)coumarin (**2b**)*

Yield 25%; mp 168–169 °C. ^{1}H NMR (300 MHz) ($CDCl_3$): $\delta = 3.87$ (s, 3H), 6.85 (m, 2H), 7.36 (dd, $J = 5.0$; 3.0 Hz, 1H), 7.42 (d, $J = 8.4$ Hz, 1H), 7.50 (dd, $J = 5.0$; 1.2 Hz, 1H), 7.87 (s, 1H), 8.11(dd, $J = 3.0$; 1.2 Hz, 1H). ^{13}C NMR (75.4 MHz) ($CDCl_3$): $\delta = 55.7, 100.3, 112.8, 113.0, 119.3, 125.0, 125.5, 126.0, 128.6, 134.6, 137.5, 154.6, 160.8, 162.4$. EI-MS ($m/z$): 259 $[M + 1]^+$, 258 $[M^+]$. Anal. Calcd. for $C_{14}H_{10}O_3S$: C 65.10, H 3.90; Found: C 65.15, H 3.97.

*4.2.7. 3-(Indol-3-yl)-7-methoxycoumarin (**2c**)*

Yield 29%; mp 185–186 °C. ^{1}H NMR (75.4 MHz) ($CDCl_3$): $\delta = 3.95$ (s, 3H), 6.89 (m, 2H), 7.28 (m, 2H), 7.47 (m, 2H), 7.95 (m, 1H), 8.10 (s, 1H), 8.13 (d, $J = 3.0$ Hz, 1H), 8.57 (br, 1H). ^{13}C NMR (300 MHz) ($CDCl_3$): $\delta = 55.7, 100.3, 100.0, 111.7, 112.6, 113.6, 119.4, 119.5, 120.6, 122.5, 126.0, 126.8, 128.1, 135.5, 136.2, 153.8, 161.1, 161.6$. EI-MS ($m/z$): 292 $[M + 1]^+$, 291 $[M^+]$. Anal. Calcd. for $C_{18}H_{13}NO_3$: C 74.22, H 4.50; Found: C 74.29, H 4.56.

*4.2.8. 6-Methoxy-3-(thiophen-2-yl)coumarin (**3a**)*

Yield 47%; mp 150–151 °C. ^{1}H NMR (300 MHz) ($CDCl_3$): $\delta = 3.85$ (s, 3H), 6.96 (d, $J = 2.8$ Hz, 1H), 7.09 (m, 2H), 7.27 (d, $J = 9.0$ Hz, 1H), 7.42 (dd, $J = 5.1$; 1.0 Hz, 1H), 7.79 (dd, $J = 3.7$; 1.0 Hz, 1H), 7.94 (s, 1H). ^{13}C NMR (75.4 MHz) ($CDCl_3$): $\delta = 55.7, 109.4, 117.3, 119.0, 119.6, 121.9, 127.0, 127.5, 127.7, 135.2, 135.9, 147.1, 156.2, 161.1$. EI-MS ($m/z$): 259 $[M + 1]^+$, 258 $[M^+]$. Anal. Calcd. for $C_{14}H_{10}O_3S$: C 65.10, H 3.90; Found: C 65.15, H 3.94.

*4.2.9. 6-Methoxy-3-(thiophen-3-yl)coumarin (**3b**)*

Yield 43%. mp 164–165 °C. ^{1}H NMR (300 MHz) ($CDCl_3$): $\delta = 3.84$ (s, 3H), 6.95 (d, $J = 3.0$ Hz, 1H), 7.06 (dd, $J = 9.0$; 3.0 Hz, 1H), 7.25 (d, $J = 9.0$ Hz, 1H), 7.37 (dd, $J = 5.1$; 3.0 Hz, 1H), 7.50 (dd, $J = 5.1$; 1.3 Hz, 1H), 7.86 (s, 1H), 8.18 (dd, $J = 3.0$; 1.3 Hz, 1H). ^{13}C NMR (75.4 MHz) ($CDCl_3$): $\delta = 55.7, 109.6, 117.2, 118.9, 119.7, 122.8, 125.6, 126.0, 126.1, 134.3, 136.9, 147.2, 156.0, 160.1$. EI-MS ($m/z$): 259 $[M + 1]^+$, 258 $[M^+]$. Anal. Calcd. for $C_{14}H_{10}O_3S$: C 65.10, H 3.90; Found: C 65.20, H 3.99.

*4.2.10. 3-(Indol-3-yl)-6-methoxycoumarin (**3c**)*

Yield 38%; mp 188–189 °C. ^{1}H NMR (300 MHz) ($CDCl_3$): $\delta = 3.84$ (s, 3H), 5.87 (d, $J = 7.7$ Hz, 1H), 6.93 (d, $J = 2.8$ Hz, 1H), 7.04 (dd, $J = 9.0$; 2.8 Hz, 1H), 7.30 (m, 3H), 7.79 (d, $J = 7.7$ Hz, 1H), 8.01 (s, 1H), 8.27 (s, 1H), 8.30 (br, 1H). ^{13}C NMR (75.4 MHz) ($CDCl_3$): $\delta = 55.7, 109.3, 112.6, 115.4, 117.2, 118.7, 119.3, 119.8, 122.7, 124.6, 125.7, 127.3, 135.9, 137.0, 146.7, 150.8, 156.1, 160.5$. EI-MS ($m/z$): 292 $[M + 1]^+$, 291 $[M^+]$. Anal. Calcd. for $C_{18}H_{13}NO_3$: C 74.22, H 4.50; Found: C 74.30, H 4.52.

*4.2.11. 5,7-Dimethoxy-3-(thiophen-2-yl)coumarin (**4a**)*

Yield 45%; mp 177–178 °C. ^{1}H NMR (300 MHz) ($CDCl_3$): $\delta = 3.86$ (s, 3H), 3.93 (s, 3H), 6.31 (d, $J = 2.1$ Hz, 1H), 6.46 (d, $J = 2.1$ Hz, 1H), 7.10 (dd, $J = 5.0$; 3.6 Hz, 1H), 7.36 (d, $J = 5.0$ Hz, 1H), 7.72 (d, $J = 3.6$ Hz, 1H), 8.29 (s, 1H). ^{13}C NMR (75.4 MHz) ($CDCl_3$): $\delta = 55.6, 56.0, 92.4, 95.1, 126.5, 127.1, 127.3, 127.5, 131.5, 136.9, 153.2, 155.3, 156.9, 160.0, 163.4$. EI-MS ($m/z$): 289 $[M + 1]^+$, 288 $[M^+]$. Anal. Calcd. for $C_{15}H_{12}O_4S$: C 62.49, H 4.20; Found: C 62.55, H 4.27.

*4.2.12. 5,7-Dimethoxy-3-(thiophen-3-yl)coumarin (**4b**)*

Yield 35%; mp 158–159 °C. ^{1}H NMR (300 MHz) ($CDCl_3$): $\delta = 3.85$ (s, 3H), 3.90 (s, 3H), 6.28 (d, $J = 1.8$ Hz, 1H), 6.42 (d, $J = 1.8$ Hz, 1H), 7.35 (dd, $J = 4.8$; 2.5 Hz, 1H), 7.52 (d, $J = 4.8$ Hz, 1H), 8.10 (d, $J = 2.5$ Hz, 1H), 8.20 (s, 1H). ^{13}C NMR (75.4 MHz) ($CDCl_3$): $\delta = 55.6, 55.8, 92.2, 94.8, 104.3, 117.3, 124.4, 125.2, 126.1, 132.7, 135.0, 155.3, 156.8, 160.4, 163.2$. EI-MS ($m/z$): 289 $[M + 1]^+$, 288 $[M^+]$. Anal. Calcd. for $C_{15}H_{12}O_4S$: C 62.49, H 4.20; Found: C 62.53, H 4.24.

*4.2.13. 5,7-Dimethoxy-3-(indol-3-yl)coumarin (**4c**)*

Yield 43%; mp 179–180 °C. ^{1}H NMR (300 MHz) ($CDCl_3$): $\delta = 3.88$ (s, 3H), 3.95 (s, 3H), 5.68 (d, $J = 7.2$ Hz, 1H), 6.33 (d, $J = 2.0$ Hz, 1H), 6.48 (d, $J = 2.0$ Hz, 1H), 7.33 (m, 2H), 7.89 (dd, $J = 7.2$; 1.2 Hz, 1H), 8.17 (s, 1H), 8.33 (dd, $J = 7.0$; 1.2 Hz, 1H), 8.48 (br, 1H). ^{13}C NMR (75.4 MHz) ($CDCl_3$): $\delta = 55.8, 56.0, 92.3, 95.0, 104.6, 113.6, 115.3, 115.8, 119.6, 122.6, 124.5, 127.6, 133.3, 136.0, 151.0, 155.0, 156.8, 161.1, 163.2$. EI-MS ($m/z$): 322 $[M + 1]^+$, 321 $[M^+]$. Anal. Calcd. for $C_{19}H_{15}NO_4$: C 71.02, H 4.71; Found: C 71.10, H 4.77.

4.3. Determination of MAO isoforms activity

The effects of the new synthesized compounds on hMAO isoform enzymatic activity were evaluated by a fluorimetric method following the experimental protocol previously described by us [15].

Briefly, 0.1 mL of sodium phosphate buffer (0.05 M, pH 7.4) containing the test drugs (new compounds or reference inhibitors) in various concentrations and adequate amounts of recombinant hMAO-A or hMAO-B required and adjusted to obtain in our experimental conditions the same reaction velocity, (hMAO-A: 1.1 μg protein; specific activity: 150 nmol of *p*-tyramine oxidized to *p*-hydroxyphenylacetaldehyde/min/mg protein; hMAO-B: 7.5 μg protein; specific activity: 22 nmol of *p*-tyramine transformed/min/mg protein) were incubated for 15 min at 37 °C in a flat-black-bottom 96-well microtest™ plate, placed in the dark fluorimeter chamber. After this incubation period, the reaction was started by adding (final concentrations) 200 μM Amplex® Red reagent, 1 U/mL horseradish peroxidase and 1 mM *p*-tyramine. The production of H_2O_2 and, consequently, of resorufin was quantified at 37 °C in a multidetection microplate fluorescence reader (FLX800™, Bio-Tek® Instruments, Inc., Winooski, VT, USA) based on the fluorescence generated (excitation, 545 nm, emission, 590 nm) over a 15 min period, in which the fluorescence increased linearly.

Control experiments were carried out simultaneously by replacing the test drugs (new compounds and reference inhibitors) with appropriate dilutions of the vehicles. In addition, the possible capacity of the above test drugs to modify the fluorescence generated in the reaction mixture due to non-enzymatic inhibition (e.g., for directly reacting with Amplex® Red reagent) was determined by adding these drugs to solutions containing only the Amplex® Red reagent in a sodium phosphate buffer.

The specific fluorescence emission (used to obtain the final results) was calculated after subtraction of the background activity, which was determined from vials containing all components except the hMAO isoforms, which were replaced by a sodium phosphate buffer solution.

4.4. Ligand docking

All docking calculations were performed with Maestro 9.0 package [34]. The crystal structure of hMAO-B was prepared for

docking with the Protein Preparation Wizard workflow of Maestro that allows adding hydrogens which were subsequently minimized with OPLS_2005 force field, and also optimize the protonation state of His residues and the orientation of hydroxyl groups, Asn residues, and Gln residues. The docking was performed by means of the Schrödinger program Glide [35], treating the ligands with a fully flexible all-atom representation, and the receptor with a rigid grid depiction. The grid was generated by applying a van der Waals radii scaling factor of 1.00 with a partial charge cut-off of less than 0.25*e*. The co-crystal ligand was used to center docking box with a size capable of accommodating ligands with a length of $\leq$20 Å. Before docking calculations, all the compounds were subjected to ligand preparation with the LigPrep tool of Maestro [34]. Different protonation states using a pH value of 7.0 ± 2.0 and tautomers were generated. The docking calculations were performed with Glide extra precision (XP) mode. A post-docking minimization was made on the output complexes in order to reduce the initial 25 poses per ligand to 5. During the eMBrAcE calculation the initial Glide XP binding poses were subjected to a minimization using a OPLS_2005 force field. Only residues inside a 5 Å shell from the ligand were allowed to move freely, residues outside this shell were frozen.

Acknowledgments

This work was partially supported by grants from Xunta de Galicia (Spain; PGIDIT09CSA030203PR and 10PXIB203303PR), University of Cagliari (ex 60% 2009), Fondazione Banco Sardegna 2007 and MIUR 2008.

E. Quezada thanks for a postdoctoral grant from FCT (Portugal). G. Ferino is grateful to Regione Autonoma della Sardegna for a Master & Back scholarship. Authors thanks S. Vilar for helpful suggestions on the docking experiments. Technical support from Red Gallega de Boinformatica and Centro de Supercomputacion de Galicia (CESGA) is gratefully acknowledged.

References

[1] M. Reyes-Parada, A. Fierro, A.P. Iturriaga-Vasquez, B.K. Casseis, Curr. Enzyme Inhib. 1 (2005) 85–95.
[2] J. Grimsby, N.C. Lan, R. Neve, K. Chen, J.C. Shih, J. Neurochem. 55 (1990) 1166–1169.
[3] S.E. Rigby, J. Basran, J.P. Combe, A.W. Mohsen, H. Toogood, A. van Thiel, M.J. Sutcliffe, D. Leys, A.W. Munro, N.S. Scrutton, Biochem. Soc. Trans. 33 (part 4) (2005) 754–757.
[4] D.E. Edmondson, A. Mattevi, C. Binda, M. Li, F. Hubalek, Curr. Med. Chem. 11 (2004) 1983–1993.
[5] J.J. Chen, D.M. Swope, K. Dashtipour, Clin. Ther. 29 (2007) 1825–1849.
[6] P. Pacher, V. Kecskeméti, Curr. Med. Chem. 11 (2004) 925–943.
[7] C. Binda, P. Newton-Winson, F. Hubálek, D.E. Edmonson, A. Mattevi, Nat. Struct. Biol. 9 (2002) 22–26 Data deposition. www.pdb.org (PDB ID code 1GOS).
[8] C. Binda, J. Wang, L. Pisani, C. Caccia, A. Carotti, P. Salvati, D.E. Edmondson, A. Mattevi, J. Med. Chem. 50 (2007) 5848–5852.
[9] C. Gnerre, M. Catto, F. Leonetti, P. Weber, P.A. Carrupt, C. Altomare, A. Carotti, B. Testa, J. Med. Chem. 43 (2000) 4747–4758.
[10] F. Chimenti, D. Secci, A. Bolasco, P. Chimenti, A. Granese, O. Befani, P. Turini, S. Alcaro, F. Ortuso, Bioorg. Med. Chem. Lett. 14 (2004) 3697–3703.
[11] M.J. Matos, D. Viña, E. Quezada, C. Picciau, G. Delogu, F. Orallo, L. Santana, E. Uriarte, Bioorg. Med. Chem. Lett. 19 (2009) 3268–3270.
[12] M.J. Matos, D. Viña, C. Picciau, F. Orallo, L. Santana, E. Uriarte, Bioorg. Med. Chem. Lett. 19 (2009) 5053–5055.
[13] M.J. Matos, D. Viña, P. Janeiro, F. Borges, L. Santana, E. Uriarte, Bioorg. Med. Chem. Lett. 20 (2010) 5157–5160.
[14] S.P. Kamat, S.K. Paknikar, P.S. Beaucahmp, J. Chem. Res. (S) (2002) 242–246.
[15] N. Hans, M. Singhi, V. Sharma, S.K. Grover, Indian J. Chem. 35B (1996) 1159–1162.
[16] W.H. Perkin, J. Chem. Soc. 21 (1868) 53–63.
[17] W.H. Perkin, J. Chem. Soc. 31 (1877) 388–427.
[18] L. Santana, H. González-Díaz, E. Quezada, E. Uriarte, M. Yañez, D. Viña, F. Orallo, J. Med. Chem. 51 (2008) 6740–6751.
[19] H.M. Berman, J. Westbrook, Z. Feng, G. Gilliland, T.N. Bhat, H. Weissig, I.N. Shindyalov, P.E. Bourne, Nucleic Acids Res. 28 (2000) 235–242.
[20] D. Tarasov, D. Tovbin, J. Mol. Model. 15 (2009) 329–341.
[21] S. Vilar, G. Cozza, S. Moro, Curr. Top. Med. Chem. 8 (2008) 1555–1572.
[22] S. Vilar, J. Karpiak, S. Costanzi, J. Comput. Chem. 31 (2010) 707–720.
[23] G.L. Warren, C.W. Andrews, A.M. Capelli, B. Clarke, J. Lalonde, M.H. Lambert, M. Lindvall, N. Nevins, S.F. Semus, S. Senger, G. Tedesco, I.D. Wall, J.M. Woolven, C.E. Peishoff, M.S. Head, J. Med. Chem. 49 (2006) 5912–5931.
[24] S. Costanzi, I.G. Tikhonova, M. Ohno, E.J. Roh, B.V. Joshi, A.O. Colson, D. Houston, S. Maddileti, T.K. Harden, K.A. Jacobson, J. Med. Chem. 50 (2007) 3229–3241.
[25] J.J. Irwin, B.K. Shoichet, J. Chem. Inf. Model. 45 (2005) 177–182.
[26] A.P. Bradley, Pattern Recognit. 30 (1997) 1145–1159.
[27] J.A. Hanley, B.J. Mcneil, Radiology 143 (1982) 29–36.
[28] B.J. Mcneil, J.A. Hanley, Med. Decis. Making 4 (1984) 137–150.
[29] Macro Model Version 9.1. Schrödinger, LLC, New York, NY, 2009.
[30] A. Sahoo, S. Yabanoglu, B.N. Sinha, G. Ucar, A. Basu, V. Jayaprakash, Bioorg. Med. Chem. Lett. 20 (2010) 132–136.
[31] F. Chimenti, E. Maccioni, D. Secci, A. Bolasco, P. Chimenti, A. Granese, O. Befani, P. Turini, S. Alcaro, F. Ortuso, R. Cirilli, F. La Torre, M.C. Cardia, S. Distinto, J. Med. Chem. 48 (2005) 7113–7122.
[32] Y. Ming, D.W. Boykin, Heterocycles 26 (1987) 3229–3231.
[33] R.R. Roberts, J.G. Bentsen, Y. Li, U.S. Pat. Appl. Publ. (2004) US 2004062930.
[34] Maestro Version 9.0. Schrödinger, LLC, New York, NY, 2009.
[35] Glide Version 5.5. Schrödinger, LLC, New York, NY, 2009.